XIX IMEKO World Congress
Fundamental and Applied Metrology
September 6–11, 2009, Lisbon, Portugal

NONDESTRUCTIVE EVALUATION OF PLEXIGLAS MATERIALS USING LOCK-IN AND PULSE PHASE INFRARED THERMOGRAPHY

R. Montanini [1], *S. Aliquò* [1]

[1] Faculty of Engineering, University of Messina, Messina, Italy, rmontanini@ingegneria.unime.it

Abstract – Lock-in and pulse phase infrared thermography measurement techniques have been exploited for quantitative assessment of subsurface defects in a reference specimen made of Plexiglas. Radiometric thermal images were post-processed using a contrast approach in the frequency domain, allowing defect depth location to be resolved with a relative combined standard uncertainty of about 7% for thicknesses above 3 mm. Conversely, significant radial heat diffusion next to the boundary of the discontinuity made accurate sizing of deeper subsurface defects more difficult. The obtained results demonstrate the potentiality of active thermography as a fast, powerful contactless NDT measurement tool.

Keywords: Temperature measurements, radiometric infrared thermography, non destructive testing (NDT)

1. INTRODUCTION

Total quality is now an established concept for mass products such as cars, consumer electronics, and personal computers. In many fields, primarily aerospace and military, it has been the rule for years, for security reasons. A major effort to reach this quality concept is to implement inspection tasks along the production line through effective nondestructive testing (NDT) methods to be used for either acceptance/rejection of parts, or for inspection of end products in service [1].

In recent years, remarkable progresses in high sensitive infrared image detectors and much effort from researchers in leading university laboratories have brought about fast growth of infrared radiometric measurement techniques. Nowadays, active thermography [2-7] is recognized as one of the most powerful NDT tool to detect flaws and defects in different kinds of materials, such as metals, composites, and polymers. The active approach involves using an excitation source to induce thermal contrast into the material and an IR camera to measure the stationary or transient response.

In particular, lock-in thermography [8-10] makes use of modulated optical stimulation to provide information about the thermophysical properties of the material as well as to identify subsurface defects in a quick and contactless way. Lock-in thermography has been proposed to detect areas of disbond in coatings [2], delaminations, impact damage and inclusions of spurious materials in composite materials [2,4,6], flat-bottom hole defects in steel [11-12], delaminations of veneered wood [13], to visualize fibre orientation in composites [14], to identify detachments or cracks in frescoes [15-17]. One limitation of lock-in thermography lies on the available range of frequencies for the heat flux modulation, which may be not sufficiently low to detect deeper defects in materials of very low thermal diffusivity and/or large thickness.

Another approach is pulse thermography, which can be obtained by stimulating the part with one or more pulsed heat sources and monitoring its surface temperature evolution during the transient heating (cooling) phase [3,6,11,15,16]. The visibility of defects depends on several factors, which include material characteristics (i.e. thermal contrast), atmospheric conditions and instrument sensitivity. Measurements performed by means of the pulsed thermographic method are affected by local variation of the emissivity coefficient and by non-uniform heating of the surface, that can mask the defect visibility. The emissivity problem may be overcome by painting the surface, but this could be a solution only for parts where this surface finish is tolerable. The uniformity of surface heating may be improved by using the lateral heating technique described by Grinzato et al [17].

A measurement technique which combines the advantages of both lock-in and pulse thermography without sharing their drawbacks is pulse phase termography, which has been first proposed by Maldague and Marinetti [18-19]. The specimen is pulse heated as in pulsed thermography and the mix of frequencies of the thermal waves launched into the specimen is unscrambled by computing the Fourier transform of the temperature evolution over the field of view; the phase, or magnitude, image can be presented as in modulated lock-in termography. The fact that pulse phase termography sorts available information coherently in term of frequencies brings interesting features with respect to the more traditional contrast approach used in pulse thermography.

In this paper both lock-in and pulse phase infrared thermography measurement techniques have been implemented for quantitative assessment of subsurface defects in a reference specimen made of Plexiglas. By proper post-processing of phase thermal images, size and depth locations of flat-bottom hole defects were determined and the measurement uncertainty assessed. Merits and limitations of the proposed approach, as well as metrological aspects related to possible interference inputs, are discussed thoroughly.

ISBN 978-963-88410-0-1

2. EXPERIMENTAL METHODS

All the experimental tests were performed using a 14-bit digital output infrared camera (Cedip Infrared Systems, Croissy Beaubourg, France), equipped with a high resolution (320×240 pixel) InSb focal plane array and a 25 mm optical lens. The IR camera operates in the MWIR (3-5 μm) wavelength spectral range and has a noise equivalent temperature difference (NETD) of 20 mK at 25 °C. The data acquisition system is controlled by a personal computer and allows the integration time to be varied in the range 10 μs – 5 ms, with frame rates up to 80 Hz at full resolution.

Synchronization of external analogue signals were accomplished by the lock-in module integrated into the infrared camera.

Images acquisition, camera configuration and non-uniformity correction (NUC) calculations were carried out using the DisplayIMG ver.2.6 software (Edevis GmbH, Stuttgart, Germany). Image post-processing was performed with the Labview™ ver. 8.5 software (National Instruments, Austin, Texas).

2.1. Reference specimen preparation

A reference PMMA (PolyMethylMethAcrylate) specimen, with known flat-bottom hole defects of different depth, has been prepared as shown in Fig.1. The specimen has a circular shape and presents sixteen 10 mm diameter holes, whose depth from the front side surface ranges from 0,6 mm (top right corner) to 3,6 mm (bottom left corner). The specimen front surface was painted with opaque black paint to uniform emissivity and reduce reflections.

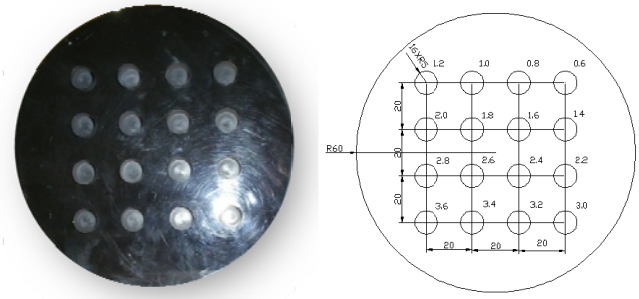

a) b)

Fig. 1. PMMA reference specimen with flat-bottom holes of different depth: a) rear side of the specimen, b) drawing showing nominal dimensions and relative position of defects.

2.2. Lock-in termography

The measuring principle used to carry out lock-in measurements is schematized in Fig. 2. The IR camera was coupled to a heat source (4×1 kW halogen lamps) which is driven by a power amplifier and a function generator. Halogen lamps were positioned so as to produce a uniform distribution of heat across the illuminated side of the specimen. The distance of the IR-camera from the sample was approximately 50 cm in order to record the entire surface of the sample. The heat source and the infrared camera signals were synchronized using a lock-in amplifier (actually integrated in the camera).

To heat the sample, a sinusoidal modulated optical wave is used, thus producing a thermal wave which propagates through the thickness of the object. As the thermal wave encounters a discontinuity it undergoes reflections because of the locally changed heat propagation parameters. The reflected wave interferes with the surface wave giving rise to a stationary oscillating temperature field, which is remotely measured through its thermal infrared emission by the IR camera. Amplitude and phase images of the reconstructed thermal wave were computed in real-time for each heat-generating frequency using the Fourier transform algorithm. These two quantities are used to present the relevant information about subsurface discontinuities. A photograph of a typical experimental set-up is shown in Fig.3.

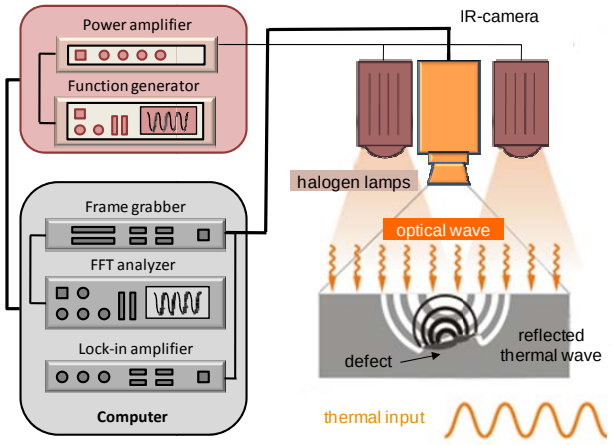

Fig. 2. Lock-in infrared thermography measuring principle.

Fig. 3. Experimental set-up for lock-in measurements.

2.3. Pulse phase thermography

The measuring principle used to carry out pulse phase measurements is schematized in Fig. 4. Instead of making use of a sinusoidal modulation, the specimen is pulse heated using either halogen lamps (long pulse > 500 ms) or high power xenon tube ring flashes (short pulse < 1 ms). Hence, thermal waves of different frequencies are launched into the

specimen simultaneously and the resulting temperature field of its surface is measured in the transient regime.

Extraction of the various frequencies was performed by acquiring sequences of images and extracting the temporal decay of each pixel in the field of view. Hence, the discrete one-dimensional Fourier transform (DFT) was applied on each pixel of the thermogram sequence to compute the real and imaginary parts and, finally, amplitude and phase images were calculated.

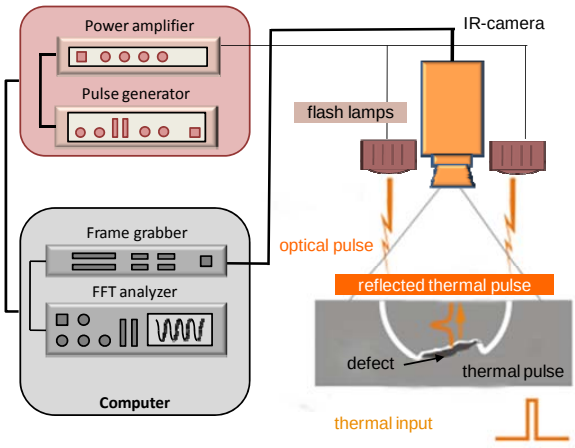

Fig. 4. Pulsed infrared thermography measuring principle.

3. RESULTS AND DISCUSSION

Lock-in amplitude and phase images of the reconstructed thermal wave on the reference specimen surface are reported in Fig. 5 for different modulation frequencies.

As it can be observed, the information given by the phase image is actually more effective, since it is relatively independent of local optical (e.g. non-uniform heating) and infrared (e.g. variability in surface emissivity) surface features. As a consequence, only signal amplitude is affected by the specimen topography while phase is not, except for the level of phase noise which of course increases in parts where less light is absorbed per unit area.

At 2,250 Hz, the relatively high modulation frequency limits the analysis to a close to the surface region, where black coating disuniformity can be appreciated in the phase image. By reducing the lock-in frequency, deeper defects are progressively revealed.

In the mid-high range (0,100 Hz < f < 0,025 Hz) the first two rows are clearly visible: in the phase images, defects appear brighter than the surrounding background and their boundaries are well defined.

The third row starts to come out for modulation frequencies in the mid-low range (0,015 Hz < f < 0,008 Hz). At this stage, the sharpness of the shallower defects in the first row becomes poor.

At 4 mHz, also the deepest flat-bottom hole is detected, although the contrast with the background is remarkably lowered due to a noteworthy reduction in the phase shift. Moreover, at very low frequency the boundary of the defects in the thermal image seems to be “out of focus”, because of significant radial heat diffusion that takes place in the specimen plane.

This frequency-dependent behaviour is a direct consequence of the inverse relationship existing between the thermal diffusion length μ and the modulation frequency f:

$$\mu = \sqrt{\frac{2k}{\rho\,\omega\,C_p}} = \sqrt{\frac{\alpha}{\pi f}} \qquad (1)$$

being $\omega = 2\pi f$, k the thermal conductivity of the material, ρ the density, C_p the specific heat at constant pressure and α the thermal diffusivity. For the amplitude image, the allowable depth range is given by (1) while, for the phase image, the maximum depth that can be inspected actually corresponds to 1,8μ [9]. Hence, usually tests should start at a quite high frequency value to investigate the surface layer; then the frequency must be decreased to investigate a deeper layer, after which the frequency must be further reduced. This procedure must go on until the entire thickness of the object is investigated or the minimum available modulation frequency is reached.

Similar results (Fig. 5, last column) were obtained by unscrambling the frequency content of the infrared images sequence measured after thermal pulse stimulation (pulse phase approach). With respect to the lock-in technique, this method can be much more fast, since it might need just one measure to analyze the whole frequency range of interest, whereas the lock-in approach requires multiple iterative tests. Phase contrast however is poorer, hiding the detection of deeper flaws. One further drawback of the pulse phase approach is that a definite temperature difference between two successive images of the sequence must exist to clearly discern defects. To display discontinuities located more in depth a higher surface heating is usually needed.

For quantitative non-destructive evaluation of subsurface defects the thermal diffusivity of the material should be known, as pointed out in (1). Unfortunately, the exact value of this parameter is not always available in the literature, because it strongly depends on the actual material composition.

To overcome this problem, a fast method which makes use of a high speed IR camera has been developed. The proposed approach is based on a transmission scheme with thermal pulse stimulation and on the well known Parker’s law [20]:

$$\alpha = 1{,}37\frac{l^2}{\pi^2\,t_{0,5}} \qquad (2)$$

where l is the material thickness and $t_{0,5}$ the half temperature rise time, that is the time needed to reach one half of the maximum temperature increment over the sample surface opposite to the heated one. A high power flash was used to generate a sudden energy pulse (to limit heat exchange with the surroundings), so that test conditions were not too dissimilar from ideal adiabatic ones.

The IR camera recorded the thermal evolution, allowing for the computation of the half temperature rise time.

The accuracy of the method can be further improved by using specific non-linear interpolation models which take into account the actual heat exchange conditions [21].

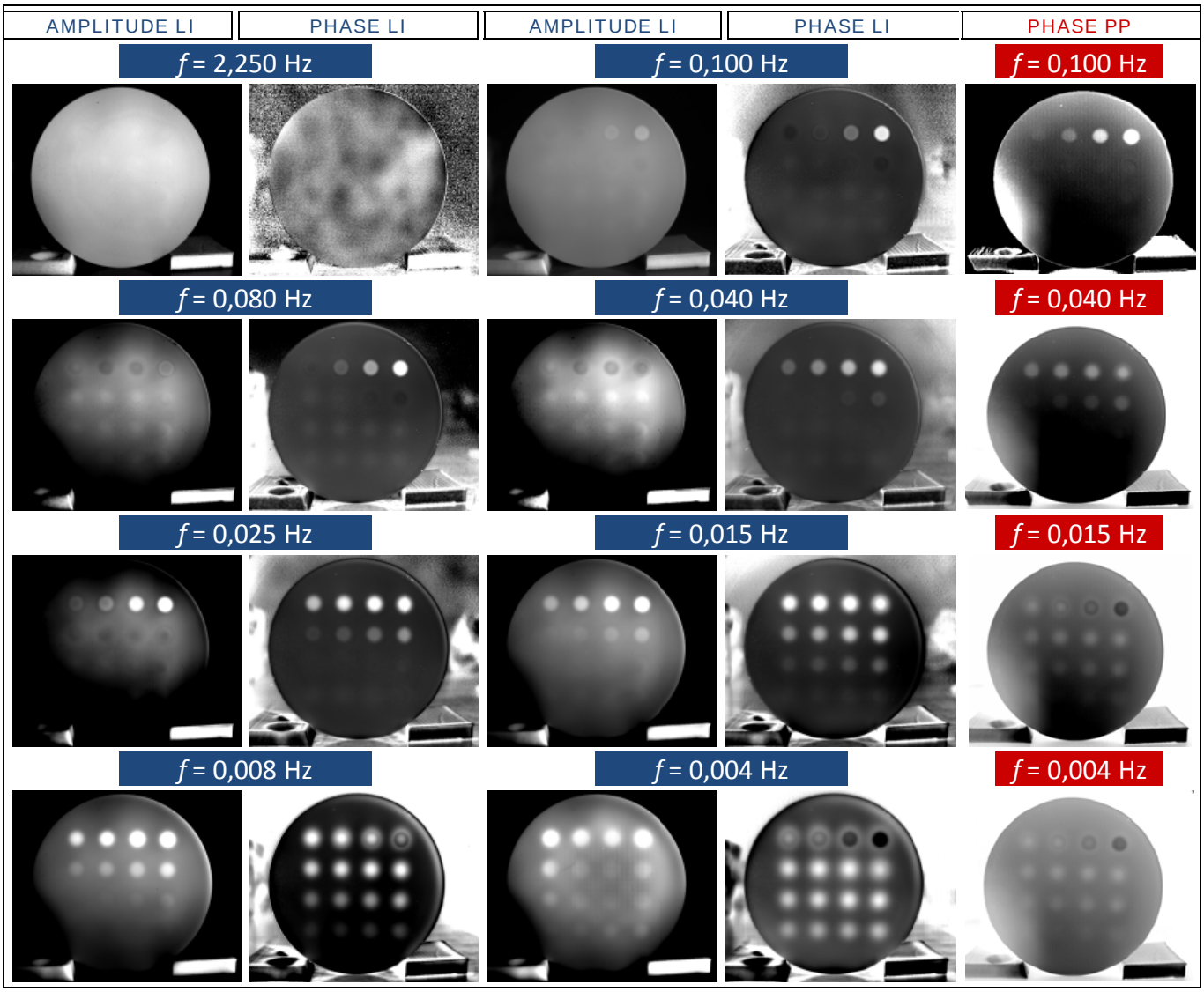

Fig. 5. Lock-in IR measurements (LI): amplitude (left) and phase (right) images of the reconstructed thermal wave on the reference specimen surface obtained at different modulation frequencies. Pulse phase IR measurements (PP): phase images obtained by unscrambling the frequency content of the infrared images sequence measured after thermal pulse stimulation using discrete Fourier transform.

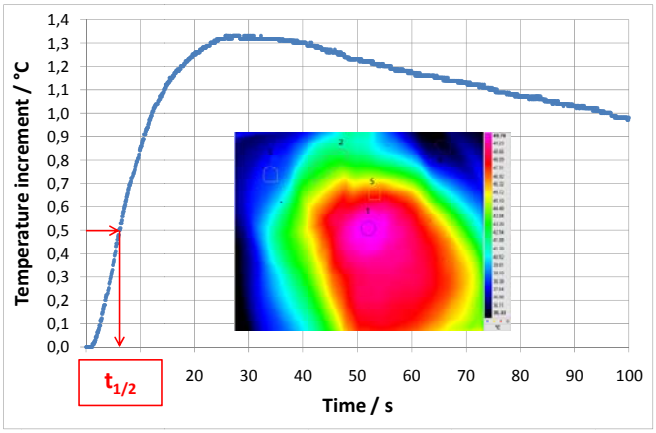

Fig. 6. Measurement of the material thermal diffusivity by means of a fast IR transient flash method: normalized temperature increments vs. heating time.

Fig. 6 shows the temperature evolution measured over a small area of a defect-free sample. It can be noted the low dispersion of the experimental data and the negative slope of the curve after the maximum temperature has been reached, due to the cooling effect. Since the measurement of the thermal transient used for the determination of the thermal diffusivity is performed by the IR camera, local values can be averaged, thus improving the S/N ratio.

According to (1) the actual depth of the defect depends upon the modulation frequency at which the defect itself is first detected.

To determine unambiguously this frequency, the normalized contrast was first defined as follows:

$$C(t) = \frac{S_{def}(t) - S_{def}(t_0)}{S_b(t_m) - S_b(t_0)} \qquad (3)$$

where S_{def} and S_b are the phase signal levels of defected and background areas, respectively, measured at time t and t_0, and t_m is the time at which the heat absorption is maximum.

Then, for each area of interest, C values at time t were plotted as a function of the modulation frequency (Fig. 7).

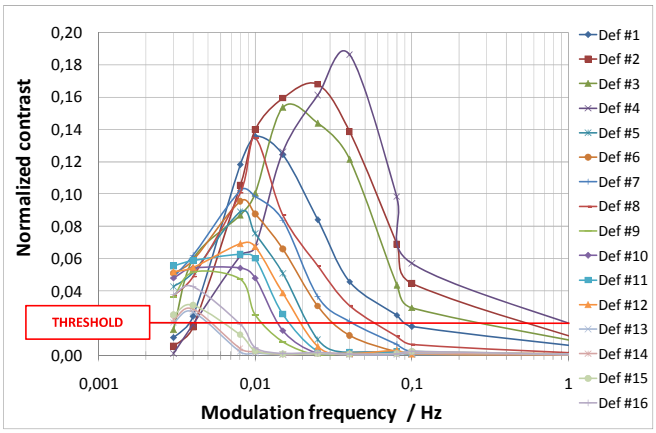

Fig. 7. Family of normalized contrast curves computed for each area of interest according to (3) vs. modulation frequency.

To determine the frequency at which each defect had been first detected (f_{TR}), a threshold level C_{TR} was defined, so that for $C \geq C_{TR}$ the discontinuity was assumed detectable, while for $C < C_{TR}$ it was not. The threshold value was determined by an iterative procedure.

Finally, the subsurface defect depth was calculated as

$$p = 1{,}8\mu = 1{,}8\sqrt{\frac{\alpha}{\pi f_{TR}}} \qquad (4)$$

Fig. 8 reports the comparison between estimated and nominal defects depth.

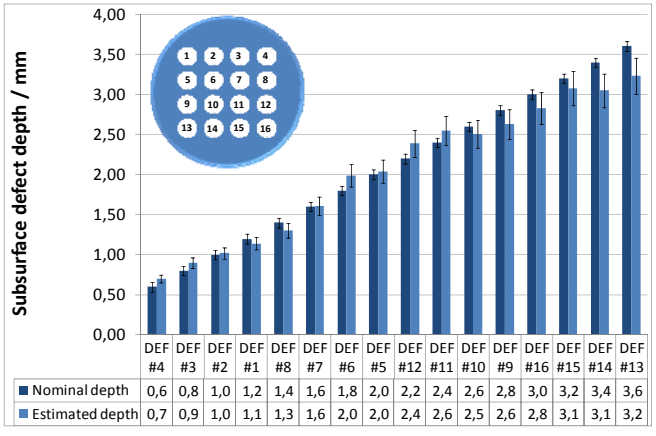

Fig. 8. Quantitative nondestructive evaluation of subsurface defects: comparison of estimated and nominal defects depth.

Uncertainty bands for nominal depth values were calculated as type B (UNI CEI ENV 13005) by assuming a rectangular distribution of width $2R$, where R = 0,05 mm is the resolution of the calliper used to measure the depth of the reference specimen flat-bottom holes. Uncertainty bands for estimated defect depth values were instead computed as combined standard uncertainty considering the type A contributions of f_{TR} and α.

Relative uncertainty of depths estimation ranges from 5,4% (defect #6) to 7,2% (defect #14). From Fig. 8 it can be observed that, as the two deepest defects are concerned, the uncertainty bands do not overlap. It can be concluded that 3,2 mm thickness roughly corresponds to the maximum detection limit for the current measurement setup.

As far as defects size assessment is concerned, obviously the best accuracy can be achieved when the contrast between defected and undefected areas is maximized.

Hence, starting from the normalized contrast vs. modulation frequency plots, the frequency f_{max} (for which it results $C = C_{max}$) was first estimated for each region of interest (Fig. 9).

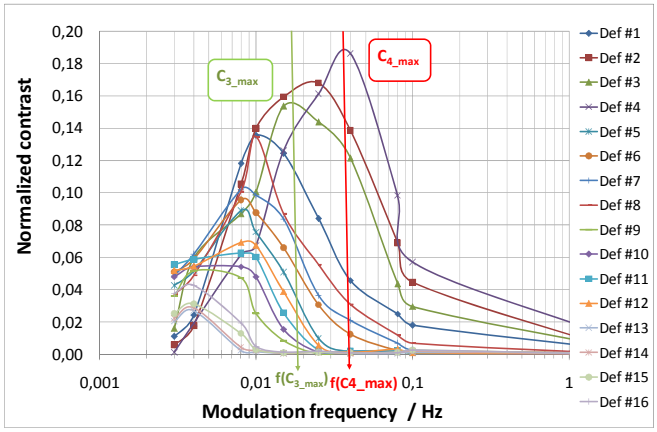

Fig. 9. Determination of the maximum normalized contrast modulation frequency for each region of interest.

Then, the nearer available (i.e., such that $f \cong f_{X\_max}$) lock-in phase image was selected. The image file was hence post-processed through different steps (filtering, image calibration, overlaying of predefined geometrical objects, measure of the defect area) by means of a dedicated digital image processing software written in Labview™.

Results are reported in Fig. 10, where they are compared with the nominal radius value.

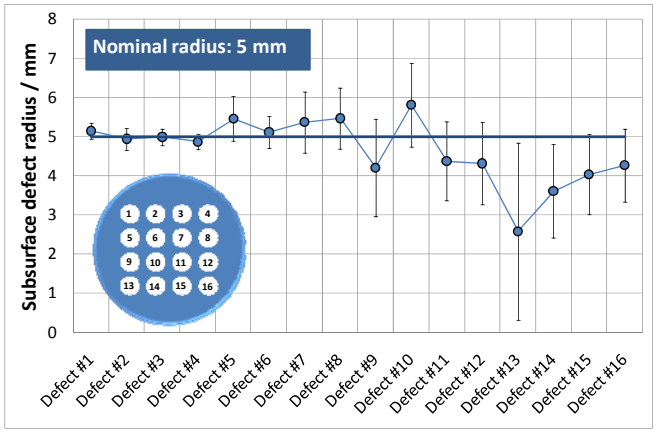

Fig. 10. Quantitative nondestructive evaluation of subsurface defects: comparison of estimated and nominal defects size.

Uncertainty bands were calculated as twice standard deviations (95% confidence value) on three measurements carried out with slightly different geometrical circles in order to take into account data variability induced by unsharpened defect boundaries.

Relative uncertainty ranges from 4,5% for the shallower defects in the first row to about 88% for the deepest one (defect #13). The relative high uncertainty found, in particular for the deeper defects (located in the lower two rows), can be attributed to the limited number of experimental data (i.e., modulation frequency steps) and to significant radial heat diffusion, that made measurement of the actual hole boundary quite difficult.

It is worth mentioning that similar results can be found by post-processing the thermograms obtained using the pulse phase approach.

4. CONCLUSIONS

Active thermography measurement techniques have been exploited for quantitative assessment of subsurface defects in a reference specimen made of Plexiglas. By proper post-processing of phase thermal images recorded at different frequencies and direct measurement of material's thermal diffusivity, a fast, contactless and effective NDT methodology has been demonstrated.

Lock-in thermography provides quantitative information about size, depth and thermal resistance of defects and, as phase images are used, relatively insensitivity to non-uniform heating and local variation of the emissivity coefficient. The main limitation of this technique lies in the minimum frequency for the heat flux modulation which may be not sufficiently low to detect deeper defects.

Pulse phase thermography is even more fast than lock-in. However, there are also some limitations: the main one is that to display deeper defects a higher surface heating is usually required, which may damage plastic materials.

Future work directions will addressed the evaluation of different types of artificial defects as well as natural ones.

ACKNOWLEDGMENTS

The authors would like to thank Prof. G. Busse and his research group at the IKP-ZfP Insitute of the University of Stuttgart (D) for their kindly support and precious advice.

REFERENCES

[1] X. Maldague, *Theory and practice of infrared technology for nondestructive testing,* John Wiley Interscience, New York, 2001.

[2] D. Wu, G. Busse, "Lock-in thermography for nondestructive evaluation of materials", *Rev. Gén. Therm.*, vol. 37, pp. 693–703, 1998.

[3] C. Meola, G.M. Carlomagno, Recent advances in the use of infrared thermography", *Meas. Sci. Technol*., vol. 15, pp. R27–R58, 2004.

[4] C. Meola, G.M. Carlomagno, A. Squillace, G. Giorleo, "Non-destructive control of industrial materials by means of lock-in thermography", *Meas. Sci. Technol*., vol. 13, pp. 1583–1590, 2002.

[5] C. Meola, G.M. Carlomagno, L. Giorleo, "The use of infrared thermography for materials characterization", *Journal of Materials Processing Technology*, vol. 155–156, pp. 1132–1137, 2004.

[6] N.P. Avdelidis, D.P. Almond, A. Dobbinson, B.C. Hawtin, C. Ibarra-Castanedo, X. Maldague, "Aircraft composites assessment by means of transient thermal NDT", *Progress in Aerospace Sciences*, vol. 40, pp. 143–162, 2004.

[7] T. Inagaki, T. Ishii, T. Iwamoto, "On the NDT and E for the diagnosis of defects using infrared thermography", *NDT&E International*, vol. 32, pp. 247–257, 1999.

[8] G.M. Carlomagno, P.G. Berardi, "Unsteady Thermo-topography in Non-Destructive Testing", *III Infrared Information Exchange*, pp. 33–40, St. Louis, Missouri, 1976.

[9] G. Busse, A. Rosencwaig, "Subsurface imaging with photoacoustics", *Appl. Phys. Lett*., vol. 36, pp. 815–16, 1980.

[10] G. Busse, D. Wu, W. Karpen, "Thermal wave imaging with phase sensitive modulated thermography", *J. Appl. Phys*., vol. 71, pp. 3962–5, 1992.

[11] T. Sakagami, S. Kubo, "Applications of pulse heating thermography and lock-in thermography to quantitative nondestructive evaluations", *Infrared Physics & Technology*, vol. 43, pp. 211–218, 2002.

[12] M. Choi, K. Kang, J. Park, W. Kim, K. Kim, "Quantitative determination of a subsurface defect of reference specimen by lock-in infrared thermography", *NDT&E International*, vol. 41, pp. 119–124, 2008.

[13] D. Wu, "Lockin thermography for defect characterization in veneered wood", *QIRT 94*, pp 298–302, Sorrento, Italy, 1994.

[14] W. Karpen, D. Wu, R. Steegmuller, G. Busse, "Depth profiling of orientation in laminates with local lock-in thermography", *QIRT 94*, pp 281–286, Sorrento, Italy, 1994.

[15] E. Grinzato, P. Bison, S. Marinetti, V. Vavilov, "Nondestructive evaluation of delaminations in fresco plaster using transient infrared termography", *Research in Nondestructive Evaluation,* vol. 5, pp. 257-274, 1994.

[16] G.M. Carlomagno, C. Meola, "Comparison between thermographic techniques for frescoes NDT", *NDT&E International*, vol. 35, pp. 559–565, 2002.

[17] E. Grinzato, P. Bison, C. Bressan, A. Mazzoldi, "NDE of frescoes by infrared thermography and lateral heating", *QIRT 98*, pp 64–70, Lodz, Poland, 1998.

[18] X. Maldague, S. Marinetti, "Pulse phase infrared thermography", *J. Appl. Phys*., vol. 79, pp. 2694–8, 1996.

[19] X. Maldague, F. Galmiche, A. Ziadi, "Advances in pulsed phase thermography", *Infrared Physics & Technology*, vol. 43, pp. 175–181, 2002.

[20] W.J. Parker, R.J. Jenkins, C.P. Butler, G.L. Abbot, "Flash method of determining thermal diffusivity", *Journal of Applied Physics,* vol.32, pp.1679–1684, 1961.

[21] E. Grinzato, S. Marinetti, "Materials NDE by non linear filtering applying heat transfer models", NATO ASI, Series E:Applied Sciences, Kluwer Academic Publishers, vol. 262, pp.117–132, 1994.